nature nanotechnology

SUPPLEMENTARY INFORMATION

DOI: 10.1038/NNANO.2010.41

Superconductivity in just four pairs of $(BETS)_2$-$GaCl_4$ molecules

K. Clark[1,2], A. Hassenien[1,3,4], S. Khan[1], K.-F. Braun[1,5], H. Tanaka[3,4], S.-W. Hla[1]

[1]Nanoscale & Quantum Phenomena Institute, Physics & Astronomy Department, Ohio University, Athens, OH 45701, USA

[2]School of Electrical Engineering & Computer Science, Ohio University, Athens, OH 45701, USA

[3]Nanotechnology Research Institute, AIST, 1-1-1 Umezono, Tsukuba, Ibaraki 305-8568, Japan

[4]JST-CREST, Kawaguchi 332-0012, Japan

[5]Physikalisch Technische Bundesanstalt, 38116 Braunschweig, Germany.

I. Synthesis and Characterization of λ-$(BETS)_2GaCl_4$

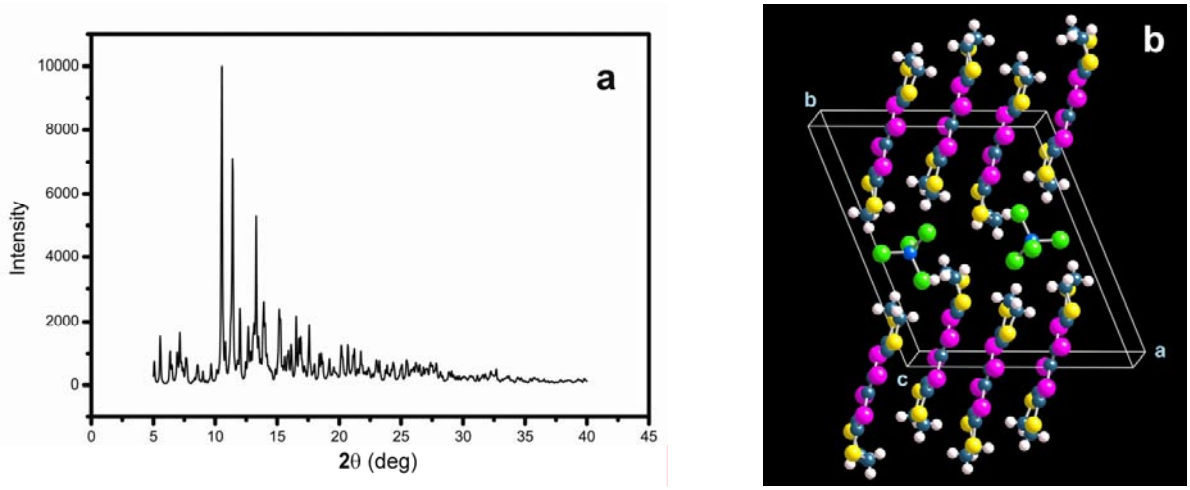

Fig. S1. a, X-ray diffraction pattern of custom synthesized λ-$(BETS)_2GaCl_4$ crystals, and **b,** the crystal structure of λ-$(BETS)_2GaCl_4$.

Needle shape single crystals of λ-$(BETS)_2GaCl_4$ have been synthesized by an electrochemical oxidation method (see methods in the manuscript for details). The x-ray diffraction measurements were carried out at room temperature using a Rigaku AFC7R diffractometer. Peaks in the diffraction pattern (Fig. S1a) indicate a triclinic crystal structure with a unit cell shown in Fig. S1b. The BETS molecules (donors) are stacked along '**a**' and '**c**' axes, and the $GaCl_4$ molecules (acceptors) are located between the BETS chains.

DOI: 10.1038/NNANO.2010.41

II. Superconducting Curve Fits

The superconducting curve fits were performed by using the formula:

$$\frac{dI}{dV} \propto \int_{0}^{2\pi}\int_{-\infty}^{\infty} \mathrm{Re}\left[\frac{|E-i\Gamma|}{\sqrt{(E-i\Gamma)^2-\Delta_0^{\,2}}}\right].f(\theta).dEd\theta$$

where $\Delta_0 = \Delta\cos 2\theta$, and $\Delta_0 = \Delta\sin 2\theta$ were used for the $d_{x^2-y^2}$ and d_{xy} symmetries, respectively[1,2]. The best curve fit was obtained using d_{xy} symmetry with θ ~ π/4, 2Δ = 12 meV, and Γ = 0.6.

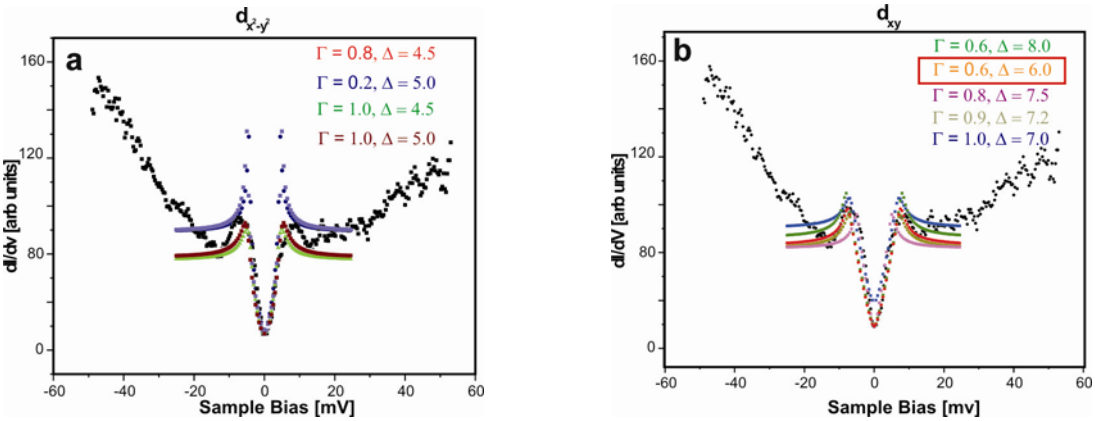

Fig. S2. Superconducting curve fittings for, **a**, $d_{x^2-y^2}$ and, **b**, d_{xy} symmetries. The best fit is the orange curve in the d_{xy} symmetry, and the corresponding Γ and Δ values are indicated with a rectangle in '**b**'.

III. Site Dependent Superconducting Gaps

We determine the site dependent superconducting gaps by positioning the STM tip on top of the BETS molecules and on the $GaCl_4$ located between the two BETS chains as indicated in fig. S3a. The dI/dV-V tunneling spectroscopy data exhibit a superconducting gap together with the two edge states on BETS chains. A superconducting gap state is still observed on $GaCl_4$ however, the two edge states in the gap have disappeared (Fig. S3b).

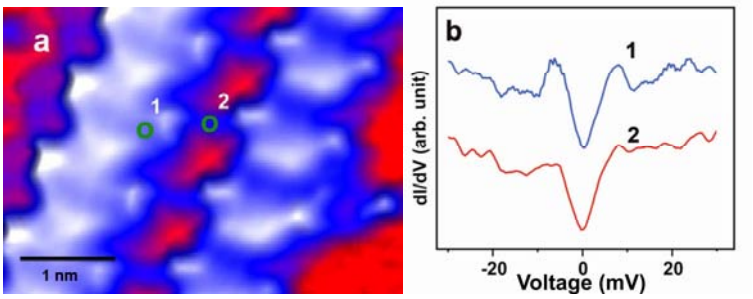

Fig. S3. a, An STM image of two BETS chains with $GaCl_4$ in between [V_t = 0.6V, I_t = 8.6x10^{-10}A], and **b**, the superconducting gaps measured on BETS and $GaCl_4$ locations indicated in '**a**' as '1' and '2', respectively.

IV. Nodal Direction

The nodal direction is oriented parallel to the '**a**' lattice vector and located between the chains as shown in Fig. S4. At these locations the superconducting coherence peaks are minimized. The antinodal states are located on top of the BETS molecules making a 45° orientation with the nodal direction.

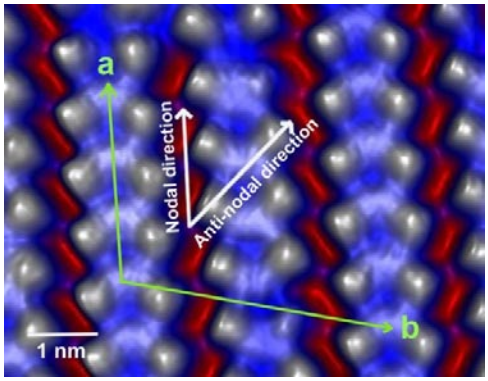

Fig. S4. An STM image of λ-$(BETS)_2GaCl_4$ molecular layer on Ag(111). The orientation of nodal and anti-nodal directions with respect to the BETS chains are indicated with white arrows. The light green arrows indicate the crystallographic '**a**' and '**b**' directions.

V. I-V Tunneling Spectroscopy of Superconducting and Metallic States

I-V and dI/dV-V tunneling spectroscopy data of molecular chains were simultaneously recorded (using a Stanford Instrument SR830 Lock-In Amplifier for the latter case) at different temperatures but at the same locations. I-V curves of molecular chains at 5.8 K exhibit a superconducting gap state around the Fermi energy, i.e. 0 mV (Fig. S5a). When the temperature was raised, this gap state disappeared in the I-V data (Fig. S5b). The I-V curve at 15K (Fig. S5b) shows a continuous increase of current as the bias is increased, indicating a metallic character.

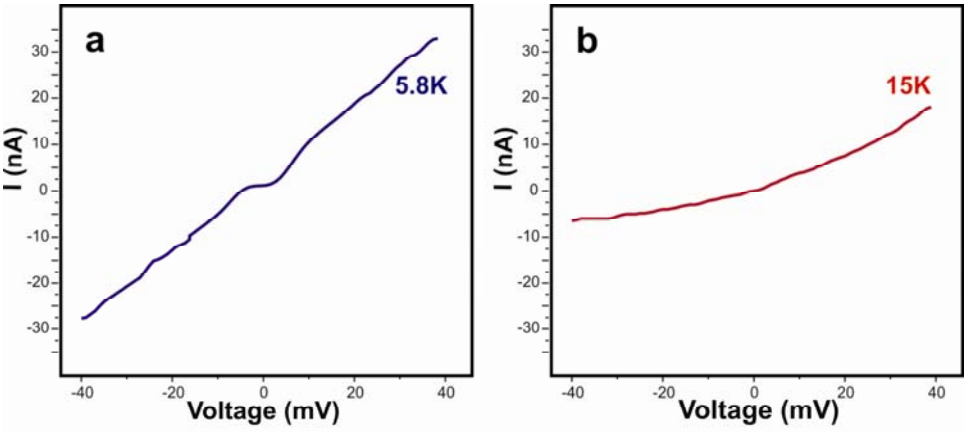

Fig. S5. I-V tunneling spectroscopy curves of superconducting (**a**), and metallic (**b**) states.

DOI: 10.1038/NNANO.2010.41

VI. Chain-Length Dependent Superconducting Gap

The dI/dV-V tunneling spectroscopy data of smaller molecular islands on Ag(111) reveal that the superconducting gap is not uniform across the islands, but it is dependent on the length of the molecular chains. Fig. S6a presents an example case. Here, the shorter chain having 12 molecular units is labeled 'S' while a longer chain located next to it composed of 14 molecular units is marked as 'L'. The dI/dV data acquired on these two chains are illustrated in Fig. S6b. Both molecular chains exhibit a superconducting gap however the longer chain has a ~7 mV gap while the neighboring shorter chain has a ~6 mV gap. Therefore, the superconducting gap observed here is dependent on the chain length.

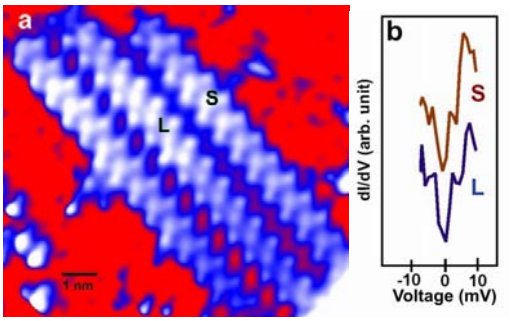

Fig. S6. a. An STM image of a smaller cluster containing three molecular chains [V_t = 0.6V, I_t = 8.6x10^{-10}A]. **b**. The averaged dI/dV data showing superconducting gaps correspond to the chains, 'L' and 'S'.

References

1. Arai, T. et al. Tunneling spectroscopy on the organic superconductor k-BEDT-TTF$_2$Cu(NCS)$_2$ using STM. *Phys. Rev. B* **63**, 104518-104522 (2001).

2. Ichimura, K. & Nomura, K. d-wave pair symmetry in the superconductivity of κ-(BEDT-TTF)$_2$X. *J. Phys. Soc. Japan* **75**, 051012 (2006).